High performance PZT based pyro-detectors with D* of 2x10^9 cmHz^{½}/W for presence, gas and spectroscopy applications.

C.Giebeler[1], J.Wright[1], S.Freeborn[1], N.Conway[1], T. Chamberlain[1], P.Clark[1], [1] Pyreos Ltd, Edinburgh, Scotland, UK
M.Schreiter[2], D. Pitzer[2], [2] Siemens AG, Munich, Germany
R.Koehler[3], [3] DIAS Infrared GmbH, Dresden, Germany

Abstract

A platform technology for low and high resolution infrared detectors has been developed. The technology is based on sputtered self-polarised lead-zirconium-titanate (PZT) films with typical film thicknesses of 200–1000 nm. These detectors are especially suited to detect radiation in the mid to far infrared wavelength range from 3-15 μm. The manufacturing process for PZT based infrared detectors is compatible with standard semiconductor/MEMS process technology which allows the easy customisation of sensor elements and results on single element, low resolution array and 1x100 line sensors are presented. The current performance of the detector elements is very good with a typical D* of 2-5x10^8 cmHz^{½}/W. In order to improve the infrared absorption coefficient from currently around 20 %, infrared absorption layers with low heat capacity have been developed that increases the IR absorption to above 90 % over the relevant wavelength range. Novel PZT based infrared detectors with integrated infrared absorption layer are expected to achieve a D* of 2x10^9 cmHz^{½}/W.

Introduction

Infra-red detectors have traditionally fallen into two separate markets and products, low cost- minimal performance detectors suitable for applications such as motion detection, and complex, costly, high performance detectors such as line arrays and focal plane arrays used in spectroscopy and IR cameras.
Ferroelectric sputtered thin films based on lead-oxide perovskites such as $Pb(Zr,Ti)O_3$ (PZT) are suitable candidates to become a platform technology to address both these markets, improving performance in the former and reducing cost in the latter. PZT is a desirable material system for mid (3-5 micron) and far (8-20 micron) infrared detection due to its high pyroelectric coefficient, low dielectric loss, high resistivity and high Curie temperature.
This is an attractive platform technology as it combines the fundamental performance parameters of the ferroelectric thin films with a MEMs/semiconductor manufacturing process, that offers the opportunity for further electronic integration, excellent device-to-device uniformity, and a cost structure that enables competitively priced commercial products.
This platform technology also provides a new level of design flexibility for uncooled-pyroelectric infrared detectors that can drive a new wave of product innovation. By using MEMs/ semiconductor process technology it is possible to create almost any size and shape of IR sensor, or sensor array. Furthermore, the detector performance can also be optimized to the market application by adjusting the physical materials/structure of the sensor element to control the heat capacity and thermal leakage into the sensor substrate, thereby allowing the detectivity to be tuned and the time constant adjusted as required.

Experimental details

The process for depositing thin ferroelectric films must produce thin, dense, homogenous and crystalline films on large substrates such as 6 or 8 inch wafers. PZT has been deposited using numerous deposition methods[1-6] but for the purpose of this paper sputtered PZT films will be discussed. The PZT films were deposited via a multi-target deposition system from metallic targets using a reactive sputtering process in an argon/oxygen environment[5]. The deposition process has been optimised to produce PZT films with a (111) orientation and high pyroelectric coefficients. PZT films are deposited onto a metallic bottom electrode layer. The bottom electrode layer is deposited via a sputter process on top of a thin membrane layer that sits on top of a 6 inch silicon wafer. After the deposition of the PZT films the PZT film and the bottom electrode are patterned using standard etch processes. In a next step the top electrode layer and the contact lines are deposited to finish the device built.
To increase the infrared absorption in the wavelength range from 3-15 microns two different types of absorption layers were investigated. A first approach uses a solution processable absorption layer that is spin coated onto the patterned PZT films. This absorption layer was subsequently patterned using standard patterning processes. In a second approach an absorption layer was vacuum deposited using a specialised deposition process and subsequently patterned using standard semiconductor process technology.

Results and Discussions

The data presented in figure 1 show typical x-ray diffraction results (XRD) of a 1 micron thick PZT film deposited at the optimised process temperature on to a platinum bottom electrode. The polycrystalline film shows a strong (111) texture and is free of any pyrochlore. The indicated Cu-K-beta / Cu-W-alpha-peaks are tool specific artifacts and not sample related. The films are homogenously self polarised to a high degree directly after the sputtering process, i.e. no additional poling step is required.

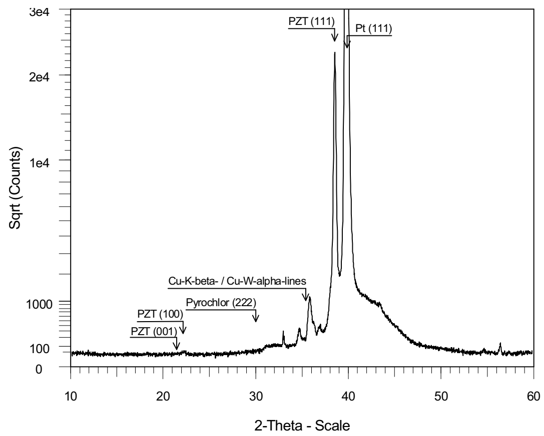

Figure 1: XRD spectrum of a typical PZT film sputtered on a platinised silicon substrate

This self-polarisation gives rise to the large pyroelectric coefficient p_k and makes sputtered PZT films especially suitable for infrared detector applications. In figure 2 the dependence of the pyroelectric coefficient p_k on the PZT film thickness is shown. The PZT film thickness was varied between 200 nm and 1400 nm. All PZT films were deposited on identical substrates under the same process conditions. The pyroelectric coefficient is highest in the 1400 nm thick film with a p_k of $2.1x10^{-4}$ C/m^2K and decreases to a p_k of 1.43 $x10^{-4}$ C/m^2K for 200 nm thick films.

Poling experiments were performed subsequently on 200 nm and 800 nm thick PZT film and the results are shown in table 1. The films were poled in a field of 20 V/µm for 5 minutes at 100 °C. The pyro-coefficient has been measured directly after the poling and after 45 minutes and no differences were detected. The change in the pyroelectric coefficient after poling is around 17 % for both films which indicate that the underlying self polarisation mechanism introduced during the sputtering process is already well developed in PZT films as thin as 200 nm. The decrease of the pyroelectric coefficient p_k with decreasing film thickness before and after poling is not yet well understood. However, it is assumed that a poorer crystallinity in thinner films caused by a more dominant influence of interfacial effects may play a role in reducing the pyroelectric coefficient in thinner PZT films.

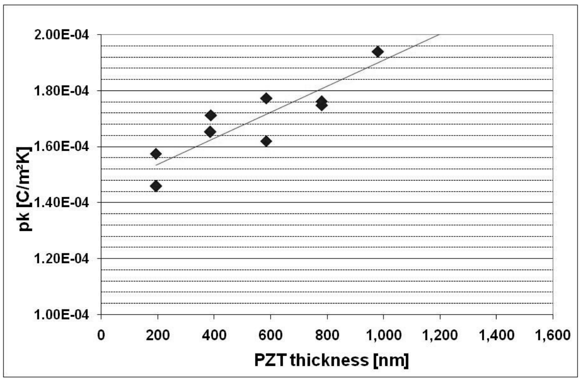

Figure 2: Thickness dependence of the pyroelectric effect in sputtered PZT films

Film Thickness [nm]	p_k (before) [C/m²K]	p_k (after) [C/m²K]
800	1.76E-4	2.08E-4
200	1.43E-4	1.66E-4

Table 1: Change in pyroelectric coefficient after poling

Further insight about the degree of self-polarisation and the switching behavior of the PZT films is obtained by measuring the slow ramp C(V) curves. During the measurement the film was first biased in the direction of the prepolarised state, i.e. the measurement starts with a negative bias sweep at the bottom electrode; it is then ramped to maximum positive bias and subsequently cycled back to the maximum negative bias. The results of the C(V) measurements for the 200 nm and 800 nm thick films are shown in figure 3.

The difference in capacitance reflects the ratios of the film thickness for these two films. With a negative bias applied the curves for both films look rather flat indicating that the applied field does not lead to a significant switching of polarisation. When a positive bias is applied a switching peak can be observed at a relatively high field strength of almost 20 V/µm for both films confirming that the polarisation introduced during the sputtering process is well established for 200 nm thick films. The large positive electric field required to switch the polarisation can be interpreted as an indication for a high internal bias found in these films which stabilises the polarisation in the direction of the prepolarised state.

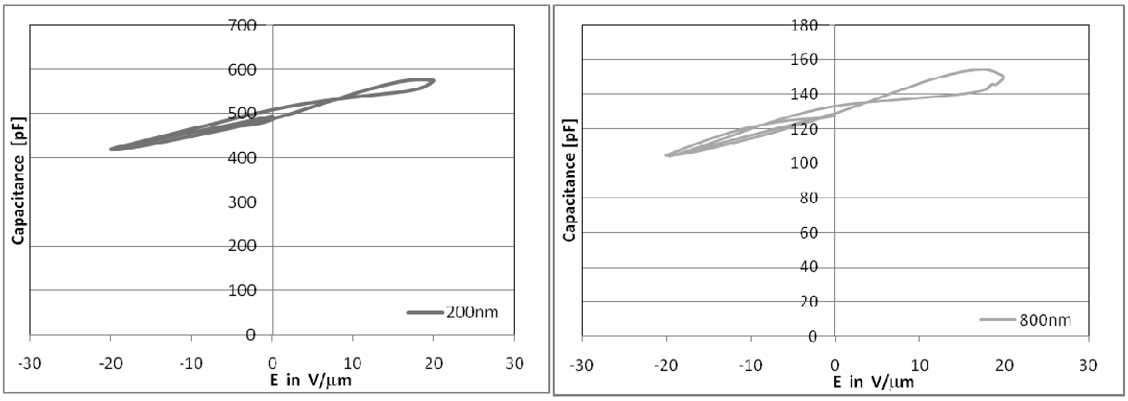

Figure 3: C(V) curves of a 200 nm and 800 nm PZT film

As outlined above the high pyroelectric coefficient in combination with the self-polarisation introduced during the deposition process makes PZT an exciting candidate for a platform technology for infrared detectors. In order to produce IR detectors reliably and reproducibly the performance of PZT film across 6 inch wafers must be very homogenous. Figure 4 exhibits uniformity data where the pyroelectric coefficient was measured at 20 positions across a 6 inch wafer and a variation of less than 5 % can be achieved. The wafer to wafer reproducibility of the PZT performance is better than 3 % during the standard manufacturing process

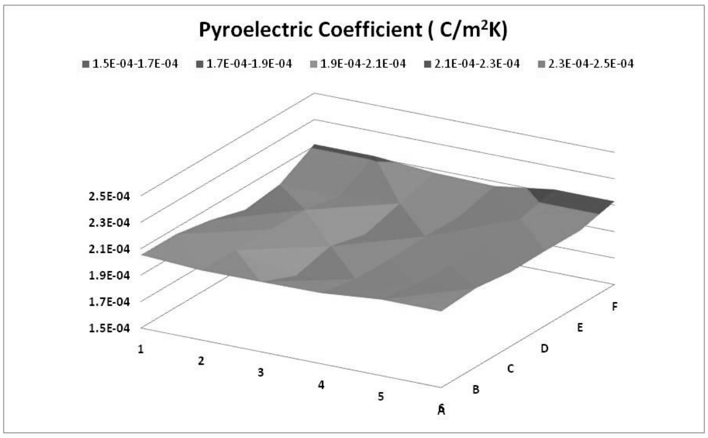

Figure 4: Typical uniformity distribution of the pyroelectric coefficient over a 6 inch wafer

As briefly mentioned above, the standard device design of an infrared detector based on self-polarised PZT films uses a thin metallic film as a top electrode and absorption layer using the standard $\lambda/4$ design approach. Infrared detectors based on this design achieve a specific detectivity D* between $2.0\text{-}5.0 \times 10^8$ $cmHz^{1/2}/W$. Comparing the experimental detector results with results from an ANSYS model of the infrared detector it is apparent that the overall absorption α of the $\lambda/4$ based device design is only around 20-30 % of the overall incident IR radiation. Increasing the infrared absorption coefficient therefore offers significant potential to further improve the device performance. The absorption spectrum of two different types of material systems is shown in figure 5. The first absorption layer is based on a commercially available graphite suspension which can be deposited via a standard spin-coating process. The second absorber layer is a vacuum deposited thin film. Both absorption layers have a heat capacity that is significantly smaller than that of a standard PZT pixel and it is therefore expected that the integration of the absorption layer will not significantly influence the device performance with respect to its frequency range.

The solution processed films show a slightly better absorbance compared to the vacuum deposited non-metallic films but both films exhibiting absorption of greater than 90 % in the relevant wavelength range. The non-linear variation of 2-4% in the absorption spectrum across the required wavelength range is not expected to have any negative effects in the targeted applications.
Sputtered PZT films clearly demonstrate the potential of becoming a platform technology for infrared detectors. The intrinsically poled films do not require any additional poling steps after deposition and the

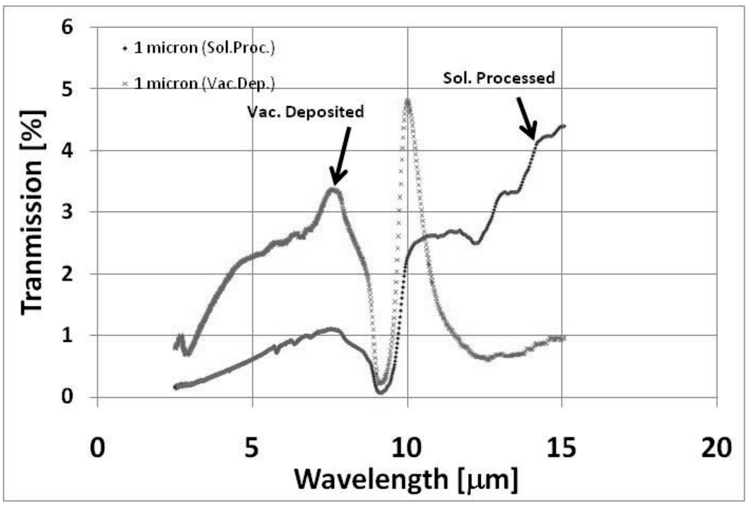

Figure 5:Transmission spectra of 1 µm thick absorption layers. One layer was produced from a solution processable material system (circles), the other was vacuum deposited (crosses)

compatibility of the manufacturing process with standard semiconductor/MEMS process technology enables the reliable and reproducible production of high performance infrared detectors. In addition the semiconductor style processing allows easy customisation of the detector elements as it only requires a mask change to create application specific detector elements.
The integration of the absorption layer with standard devices will increase the performance of infrared detectors with a specific detectivity D* significantly larger than 2.0×10^9 $cmHz^{1/2}/W$. This performance increase in combination with the possibility of producing very thin PZT films with good pyroelectric properties offers the potential for customised infrared detector solutions with a compelling price and performance.

Application results

The following section provides more application specific examples of how infrared detectors based on sputtered PZT films can be used in a variety of novel applications. As outlined above the semiconductor compatible manufacturing process allows the production of basically any pixel and array geometry with pixel sizes ranging from 20x800 µm for line sensor application to 1000x2000 µm for motion detection application. The detector elements are packaged into either standard TO cans with the first amplification stage of the electronic read out circuit integrated into the can or in customised LCC or dedicated linesensor packages. ASICs are also available for dual channel devices and linesensor applications.
Figure 6 shows examples of different detectors elements that have been produced. These range from single element devices to 4x4 arrays and line sensors. All different designs have been implemented into one multi-party mask design which allows customers to test their application specific sensor designs.

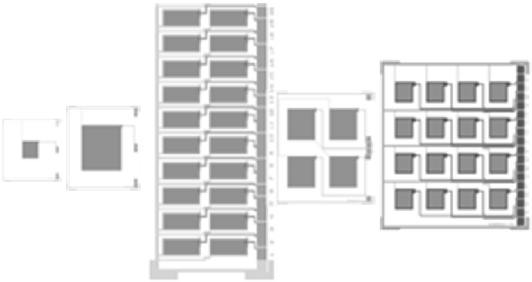

Figure 6: Examples of different PZT based IR sensor element designs. Pixel sizes vary from 200x200 to 500x500 µm

In figure 7 the device performance of a 2x2 element PZT detector is compared to a $LiTaO_3$ detector. Both detectors have an active area of 500x500 µm. The measurements were taken for both sensor types with the same source follow circuit and a black body radiation source at a temperature of 500 K. All data were corrected for the absorption of the window material.

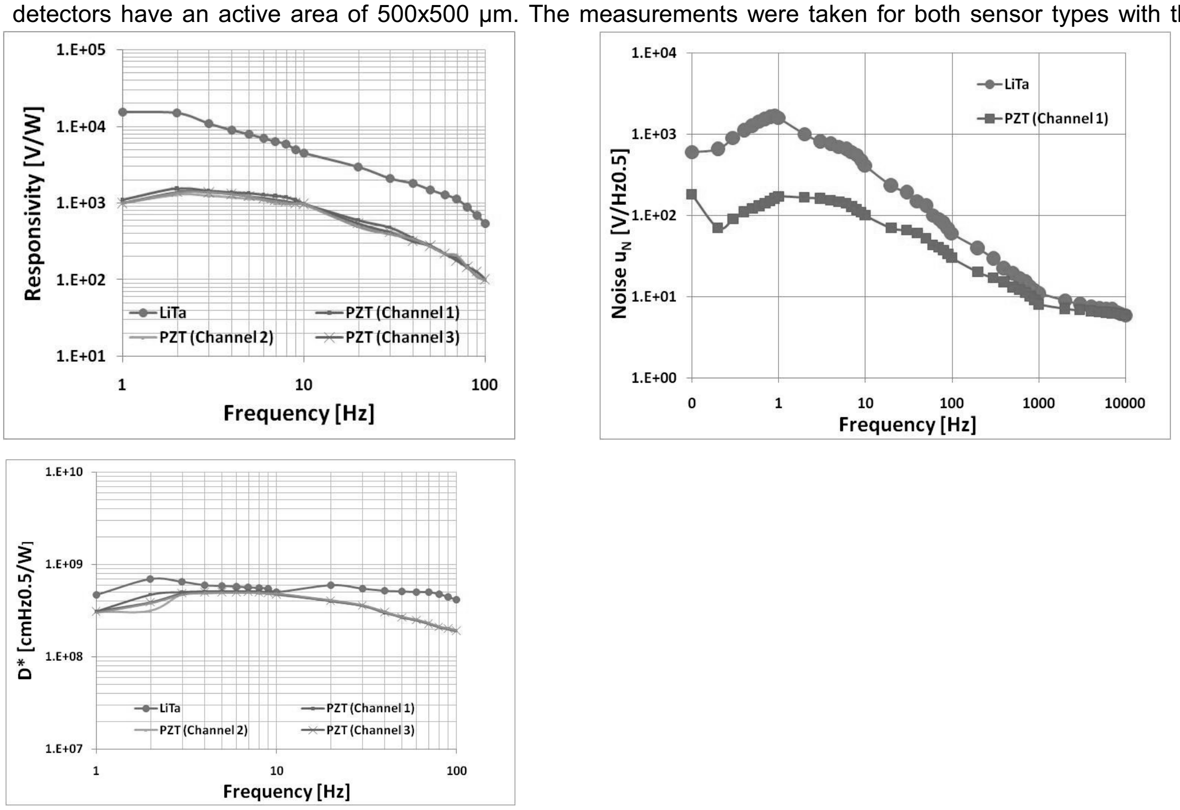

Figure 7: The left plot shows a comparison of the responsivity between the four PZT elements (solid lines) and the LiTaO3 device (circles). The right plot shows a comparison of the noise measurement between a PZT element (square) and a LiTaO3 detector (circles). The plot (bottom left) shows a comparison of the specific detectivity for PZT devices and $LiTaO_3$

The voltage responsivity as depicted in the left diagram is about a factor of six larger for the $LiTaO_3$ device compared to the PZT based device. This difference can be explained by the about five times larger dielectric constant of PZT (ε_r=270) compared to that of $LiTaO_3$ (ε_r=43). It is important to stress the nearly identical

performance of the individual channels of the PZT detector. This uniform performance is directly related to the very uniform pyroelectric coefficient across the wafer and the very good process control of any subsequent production steps.
The noise measurements (centre plot) shows significant lower noise for the PZT based devices compared to $LiTaO_3$ devices. Both sensors are dominated by the 1/f noise at higher frequency.

The plot (bottom left) shows the comparison of the specific detectivity between PZT and $LiTaO_3$ devices. Whereas the $LiTaO_3$ device exhibit a slightly larger D* at very low and at high frequencies, D* of the PZT based sensor matches that of the $LiTaO_3$ device in the frequency range of 1-10 Hz which is the relevant frequency range for almost all applications. Taken into account that the $LiTaO_3$ device absorbs about 60% of the incident IR radiation compared to only 20-30% for the PZT devices it is apparent that the PZT devices with integrated absorption layer will have a significantly better D* than that of $LiTaO_3$ devices. Improvements in the absorption will also help to improve the voltage responsivity to be comparable to that of $LiTaO_3$ devices.

Figure 8 shows a comparison of the performance of different linesensors. All three linesensors were packaged by DIAS Infrared GmbH in their standard packaging solutions and the data were read-out using dedicated ASIC solutions. All measurements were performed with a black body source at 400 °C and an infrared optics with 50 mm focal length. The modulation frequency was 128 Hz. The plot on the left shows results for a 128 pixel linesensor based on sputtered PZT films that was produced in 2001 at Siemens. The performance of the working pixels is very non-uniform and the device shows many dead pixels. The plot in the centre shows the result of the first linesensor (100 pixels) produced by Pyreos using its' optimised PZT deposition and manufacturing process. It is evident the number of non working pixels has decreased dramatically and the performance is very uniform. The slight variations between adjacent pixels are related to differences in contact line length which results in a slight reduction of the pixel sensitivity due to undesired coupling effects. The failure mode for the dead pixels in the current line sensor has been investigated and is now well understood and linesensors with 128 and 512 pixels are currently under development.

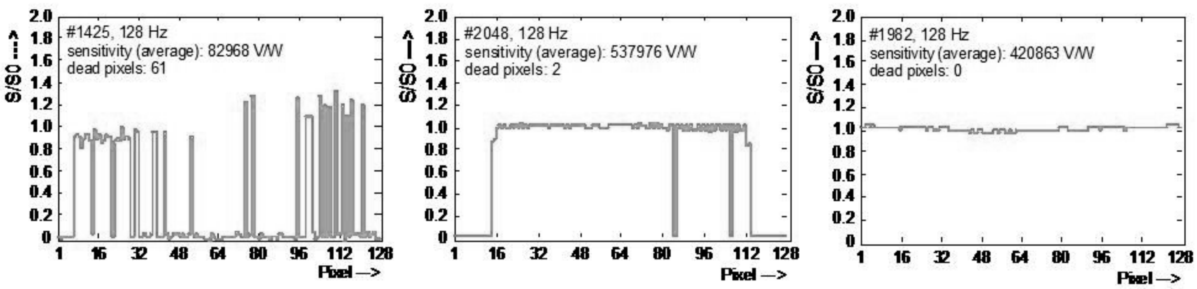

Figure 8: The left plot shows a normalised sensitivity plot for a line sensor based on sputtered PZT as produced by Siemens. The centre plot shows a normalised sensitivity plot for a line sensor based on an optimised PZT manufacturing process as produced by Pyreos. The plot on the right shows a normalised sensitivity plot for a $LiTaO_3$ based line sensor currently available from DIAS Infrared GmbH in Dresden.

The plot on the right shows the results from a commercially available LiTaO3 linesensor from DIAS Infrared GmbH. The pixel uniformity is compatible to that of the linesensor produced by Pyreos but the noise equivalent power (NEP) is approximately a factor four better 6. However, taking into account the very low IR absorption coefficient of the Pyreos' linesensor it is envisaged that by integrating it with an IR absorption layer the performance can be increased significantly to become comparable to that of currently available infrared linesensors.

Summary

The paper describes a novel platform technology for infrared detectors. The technology is based on a sputtering process that produces permanently poled PZT films directly after deposition with no need for further poling. The films are produced on standard silicon substrates and further processing is compatible with standard semiconductor/MEMs process technology which allows simple and cost-effective customisation of the sensors in terms of pixel sizes, pixel shape and pixel numbers. The performance of such sensor elements is already exceeding competing technologies and is expected to improve even further by increasing the infrared absorption of the device.

References

1. S.K. Dey and R.Zulegg, *Ferroelectrics*, **108**,37 (1990)
2. Y.Sakashita *et al*. *J.Appl.Phys.*,**69**, 8352 (1991)
3. S.B.Krupanidhi *et al*, *J.Appl.Phys.*,**71**, 376 (1992)
4. R.Bruchhaus *et a*l, *Integrated Ferroelectrics*, 1994, Vol 4, pp 365-370
5. R.Bruchhaus, et all, *Integrated Ferroelectronics*, 3:2, 151-162, 1999
6. Internal discussions with DIAS Infrared GmbH